energy&fuels

Article

pubs.acs.org/EF

Complex Flow and Composition Path in CO_2 Injection Schemes from Density Effects

Tausif Ahmed,[†] Hadi Nasrabadi,*[,†] and Abbas Firoozabadi*[,‡,§]

[†]Petroleum Engineering, Texas A&M University at Qatar, Post Office Box 23874, Doha, Qatar

[‡]Reservoir Engineering Research Institute (RERI), Palo Alto, California 94301, United States

[§]Department of Chemical Engineering, Yale University, New Haven, Connecticut 06511, United States

ABSTRACT: CO_2 injection has been used to improve oil recovery for the last 4 decades. In recent years, CO_2 injection has become more attractive because of the dual effect: injection in the subsurface (1) allows for reduction of the CO_2 concentration in the atmosphere to reduce global warming and (2) improves the oil recovery. One of the screening criteria for CO_2 injection as an enhanced oil recovery method is based on the measurement of CO_2 minimum miscibility pressure (MMP) in a slim tube. The slim tube data are used for the purpose of field evaluation and for the tuning of the equations of state. The slim tube represents one-dimensional (1D) horizontal flow. When CO_2 dissolves in the oil, the density may increase. The effect of the density increase in high-permeability reservoirs when CO_2 is injected from the top has not been modeled in the past. The increase in density changes the flow path from 1D to two-dimensional (2D) and three-dimensional (3D) (downward flow). As a result of this density effect, the compositional path in a reservoir can be radically different from the flow path in a slim tube. In this work, we study the density effect from CO_2 dissolution in modeling of CO_2 injection. We account for the increase in oil density with CO_2 dissolution using the Peng−Robinson equation of state. The viscosity is modeled based on the Pedersen−Fredenslund viscosity correlation. We perform compositional simulation of CO_2 injection in a 2D vertical cross-section with the density effect. Our results show that the density increase from CO_2 dissolution may have a drastic effect on the CO_2 flow path and recovery performance. One conclusion from this work is that there is a need to have accurate density data for CO_2/oil mixtures at different CO_2 concentrations to model properly CO_2 injection studies. Our main conclusion is that the downward flow of the CO_2 and oil mixture may not be gravity-stable, despite the widespread assumption in the literature.

INTRODUCTION

The CO_2 improved oil recovery (IOR) has been applied in petroleum production for many years. The first large-scale, commercial CO_2 IOR project began operation in 1972 at the SACROC field in west Texas and continues to this date.[1] A large number of CO_2 IOR projects have started since then; on the basis of the 2010 EOR survey by the *Oil and Gas Journal*, there are a total of 129 projects globally (120 of them in the U.S. and Canada). In the U.S. alone, CO_2 injection has accounted for the recovery of about 1.5 billion barrels of oil.[2] CO_2 injection in oil reservoirs (for sequestration purposes) has become more attractive from the standpoint of global warming concerns. The increase in the CO_2 concentration in the atmosphere because of the burning of fossil fuels and deforestation may be one of the main causes for acceleration in global warming. Because fossil fuels will be a critical component of the world energy supply for the coming decades, methods for disposal of CO_2 that do not involve long residence of CO_2 in the atmosphere (such as injection in oil and gas reservoirs) are considered as part of a possible solution.

CO_2 injection may improve oil recovery through three main mechanisms: (1) swelling, (2) reducing viscosity, and (3) decreasing residual oil saturation. Diffusion of CO_2 in the oil phase may contribute to recovery in highly heterogeneous and fractured reservoirs.[3]

In CO_2 injection schemes, the minimum miscibility pressure (MMP) from one-dimensional (1D) horizontal slim-tube measurements is often thought to be a key parameter. The MMP is defined as the minimum pressure that is required to achieve multiple contact miscibility between the injected fluid and oil at the reservoir temperature. However, the flow path may be very different in a slim tube and in a reservoir. In a slim-tube experiment, a long (10 m or longer) small diameter (0.5 cm) tube packed with sand or glass beads is saturated with oil and is then displaced by injection gas at a fixed pressure and temperature. The oil recovery after injection of some fixed amount of gas [usually 1.1 or 1.2 pore volumes (PV)] is measured at different pressures. Typically, recovery increases with an increase in the pressure and then levels off. In a recovery versus pressure plot, the MMP is usually taken to be the point where the recovery starts to level off. The measured MMP from the slim tube is used for the purpose of field evaluation or tuning equations of state.

The question is relevancy of slim-tube MMP to the performance of CO_2 injection in two-dimensional (2D) and three-dimensional (3D) reservoirs. The slim tube, because of its small diameter, represents a 1D horizontal flow. The flow in reservoir conditions, even in homogeneous domains, is 2D or 3D. As CO_2 dissolves in the oil, at certain conditions, the density increases. On the other hand, when a gas phase evolves from mixing of CO_2 and the oil, the gas phase is often lighter than CO_2 and the oil. The evolved gas phase moves upward because of buoyancy. These density effects, under the influence of gravity in

Received: March 23, 2012
Revised: May 30, 2012
Published: May 31, 2012

reservoir conditions, will change the flow path from 1D to 2D or 3D. In a 1D slim tube, there is no gravity effect.

There has been extensive research on the effect of CO_2 dissolution on oil viscosity, and many correlations have been developed. Density effects from dissolution have not been taken into account in the past; they are often ignored in modeling of CO_2 injection.[3−10] An example of neglect of the density effect is the pilot performance in the Weeks Island from CO_2 injection.[7] There was a "higher-than-expected" CO_2 production from the start with no clear explanation. Another example is an early breakthrough and high CO_2 production observed in a vertical (assumed) gravity-stable CO_2 flood in the Wellman field.[8] In this example, even significant reduction in the CO_2 injection rate did not solve the problem. The early breakthrough of CO_2 was thought to be related to gas coning. A number of other studies are based on the assumption that, when the injected CO_2 is lighter than the oil, the CO_2 injection is a stable gravity drainage process.[4−6,8,11,12] As we discuss in this work, this assumption may not be true. We point out that the CO_2 dissolution in water also results in a density increase.[13] The density increase in water is well-recognized, although it is often less than the oil density increase from CO_2 dissolution. The density increase from CO_2 dissolution in water may have a significant effect on the mixing and flow path.[14,15]

In this work, we first briefly review the literature on the change in density from CO_2 dissolution in a petroleum fluid. We then discuss how to model the increase in oil density with CO_2 dissolution (while preserving the viscosity reduction effect) using the Peng−Robinson equation of state (EOS).[16] The density effect is then examined for CO_2 injection in a 2D vertical cross-section, where we compare the results for cases with and without the density increase. We investigate the effect in (1) homogeneous 2D domains with two different permeabilities and (2) a 2D domain with random permeability distribution and anisotropic permeability.

EFFECT OF CO_2 SOLUBILITY ON OIL DENSITY

There are several published data that reveal the increase in liquid hydrocarbon density from CO_2 solubility. Lansangan and Smith[17] have found that mixtures of CO_2 and crude oil show a monotonic viscosity decrease and a density increase with an increased CO_2 concentration. They suggest that the increase in density might be caused by strong intermolecular Coulombic interactions between CO_2 and hydrocarbon molecules. There may be other explanations for the density increase.

DeRuiter et al.[18] studied the solubility and displacement of viscous crudes with CO_2 and have found that the oils exhibit an increase in density because of CO_2 solubility. The two samples in their study with American Petroleum Institute (API) gravities of 18.5° and 14° exhibited an increase in density upon CO_2 dissolution. Grigg,[19] in a study of a west Texas crude oil, observed a 2% increase in oil density after the addition of CO_2 before the phase split, while the viscosity decreased. After the phase split, the traditional viscosity−density relationship was observed; viscosity increased (decreased) when density increased (decreased).

Ashcroft and Ben-Isa[20] also reported on the effect of dissolved air, nitrogen, oxygen, methane, and carbon dioxide on the densities of liquid hydrocarbons. The hydrocarbons studied include heptane, octane, nonane, decane, dodecane, tetradecane, hexadecane, cyclohexane, methylcyclohexane, and methylbenzene (toluene). Their data show that saturation of hydrocarbon liquids with gases other than CO_2 results in a decrease of the density, while saturation with CO_2 increases the density.

DENSITY AND VISCOSITY CHANGES FROM CO_2 DISSOLUTION

As discussed earlier, there may be an increase in oil density and a decrease in viscosity with CO_2 dissolution. Lansangan and Smith[21] report density and viscosity measurement trends for oil samples from west Texas. We have selected a sample (RO-B) from Lansangan and Smith that shows an increase in density of about 5% with CO_2 dissolution in single phase. They report a density of 740 kg/m^3 and a viscosity of 0.000 77 Pa s (0.77 cP) at 11.7 MPa and 46.7 °C for the fluid before mixing with CO_2.

Using the CMG WINPROP software, we first match the density and viscosity of the oil sample by performing regression on critical properties, binary interaction coefficients, and volume shift parameters for the heavy fractions and viscosity correlation parameters. In this work, we use the Peng−Robinson EOS to calculate phase behavior and density (with volume shift parameters) and the Pedersen and Fredenslund[22] correlation to calculate viscosity. In our experience, the Pedersen and Fredenslund approach is superior to other methods for the description of viscosity of reservoir fluids in the near critical region. To improve the accuracy of predictions, we split the original C_{7+} heavy fraction (reported by Lansangan and Smith) into three pseudo-components. Table 1 lists the fluid composition with the heavy-fraction split, and Table 2 shows the measured density and viscosity with CO_2 dissolution in

Table 1. Fluid Composition (Fluid "RO-B" from Lansangan and Smith[21])

component	composition (mole fraction)
CO_2	0.0220
C_1	0.2228
C_2	0.1285
C_3	0.1235
C_4	0.0819
C_5	0.0386
C_6	0.0379
C_{7-12}	0.1301
C_{13-21}	0.1085
C_{22+}	0.1062

Table 2. Measured Density and Viscosity versus CO_2 Composition in CO_2/Oil Mixtures at 11.7 MPa and 46.7 °C (Fluid "RO-B" from Lansangan and Smith[21])

	CO_2 composition	measured viscosity ($\times 10^3$, Pa s)	measured density (kg/m^3)
		Single-Phase Region	
	0.022	0.770	0.744
	0.034	0.683	0.745
	0.1506	0.530	0.749
	0.3498	0.419	0.761
	0.5482	0.380	0.782
		Two-Phase Region	
liquid	0.5974	0.404	0.800
gas	0.7969	0.082	0.701
liquid	0.6546	0.513	0.828
gas	0.8447	0.073	0.683
liquid	0.6876	0.642	0.844
gas	0.8793	0.070	0.678
liquid	0.6981	0.787	0.856
gas	0.9040	0.069	0.674

dx.doi.org/10.1021/ef300502f | Energy Fuels 2012, 26, 4590−4598

Table 3. Fluid Critical Properties and Other Relevant Data

component	critical temperature (K)	critical pressure (atm)	molecular weight (g/mol)	acentric factor	binary interaction coefficients CO_2–x	binary interaction coefficients C_1–x
CO_2	304.2	73.76	44.01	0.2250	0.000	0.100
C_1	190.6	46.00	16.04	0.0080	0.100	0.000
C_2	305.4	48.84	30.07	0.0980	0.100	0.003
C_3	369.8	42.46	44.10	0.1520	0.100	0.009
C_4	425.2	38.00	58.12	0.1930	0.100	0.015
C_5	469.6	33.74	72.15	0.2510	0.100	0.021
C_6	507.5	32.89	86.00	0.2750	0.100	0.025
C_{7-12}	569.6	21.11	133.11	0.3462	0.069	0.038
C_{13-21}	790.3	15.00	225.57	0.4636	0.049	0.070
C_{22+}	1075.4	9.65	449.31	0.8050	0.069	0.121

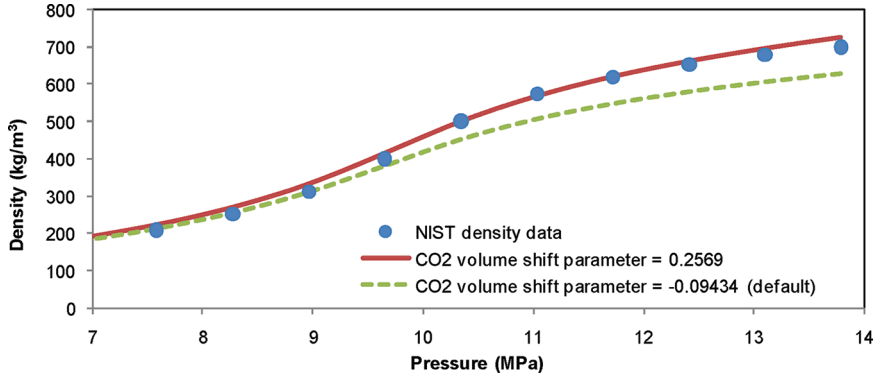

Figure 1. Density of pure CO_2 at 46.7 °C versus pressure.[25] The CO_2 densities calculated using the default volume shift parameter and our value are compared to the NIST data.

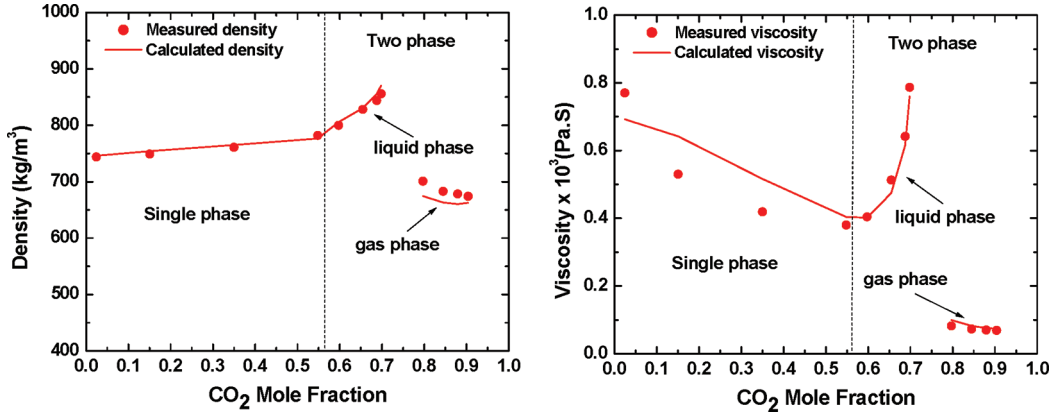

Figure 2. Variation of density and viscosity with the CO_2 mole fraction in CO_2/oil mixtures for oil "RO-B" (Table 2), with p = 11.7 MPa and T = 46.7 °C. Measured values are from Lansangan and Smith.[21] Computed density values are based on adjusted volume shift parameters.

Table 4. Volume Shift Parameters

components	CO_2 default (decrease in density with CO_2 dissolution)	CO_2 adjusted (increase in density with CO_2 dissolution)
CO_2	−0.09434	0.2569
C_1	−0.15386	−0.15386
C_2	−0.1021	−0.1021
C_3	−0.0733	−0.0733
C_4	−0.05706	−0.05706
C_5	−0.03446	−0.03446
C_6	−0.00499	−0.00499
C_{7-12}	0.2440	0.2440
C_{13-21}	0.3140	0.3140
C_{22+}	0.3416	0.3416

Table 5. Parameter Values for the Pedersen and Fredenslund[22] Viscosity Correlation

molecular-weight mixing rule coefficient	molecular-weight mixing rule exponent	coupling factor correlation coefficient	coupling factor correlation density exponent	coupling factor correlation molecular-weight exponent
0.000058	2.803	0.005456	2.0426	0.21041

single- and two-phase regions. Table 3 lists the parameters used in the EOS calculations for phase behavior.

To predict the increasing density trend, we modify the volume shift parameter of CO_2. We note that, by changing the CO_2 volume shift parameter, we can model the density increase

dx.doi.org/10.1021/ef300502f | Energy Fuels 2012, 26, 4590–4598

in the fluid from CO_2 dissolution without affecting the calculated viscosity. This is due to the fact that, in the Pedersen−Fredenslund correlation, the viscosity of the mixture depends upon the viscosity (and density) of a reference component (usually methane) and the factors that are independent of mixture density. Therefore, modifying the shift parameter of CO_2 does not affect the viscosity of the mixture.

The CO_2 density is first calculated using the Peng−Robinson EOS with the default volume shift parameter in the WINPROP. These data are compared to the isothermal CO_2 density data at 46.7 °C from the National Institute of Standards and Technology (NIST). The NIST uses an EOS developed for CO_2 by Span and Wagner,[23] with estimated density uncertainty ranging from 0.03 to 0.05%. The correlation by Jhaveri and Youngren,[24] used in many commercial simulators (including WINPROP) to calculate the volume shift parameters, may not be accurate for CO_2. The default volume shift parameter in the Jhaveri and Youngren correlation is −0.094 34, which underestimates the density as the pressure increases (Figure 1). At 11.7 MPa and 46.7 °C, we find the CO_2 volume shift parameter to be 0.2569, which is significantly different from the value by the Jhaveri and Youngren correlation (−0.094 34). Lansangan and Smith[17] report the density of pure CO_2 at the conditions of our study (46.7 °C, 11.7 MPa) to be 620 kg/m^3, which is less than the density of the oil "RO-B" (740 kg/m^3). We obtain a very good agreement with this measured value. At T = 46.7 °C and p = 11.7 MPa, our calculated value is 618 kg/m^3. In our approach to model the oil increasing density with CO_2 dissolution, we first match the oil density (without CO_2) by adjusting the volume shift parameters of the heavy fractions. Then, we use the CO_2 volume shift parameter based on the pure CO_2 density.

Table 4 lists the volume shift parameters for different components for the default case (decreasing density with CO_2 dissolution) and for the proper prediction of density (increasing density with CO_2 dissolution). Using the default CO_2 volume shift parameter gives an 11.7% difference in the value of pure CO_2 density at 11.7 MPa and 46.7 °C, as seen in Figure 1. Table 5 lists the viscosity model parameters for the Pedersen and Fredenslund[22] correlation. The results of density and viscosity predictions using parameters listed in Tables 3−5 are compared to measured values in Figure 2. The densities and viscosities shown in Figure 2 are the single-phase liquid and two-phase gas and liquid. We used measured liquid- and gas-phase compositions from Lansangan and Smith[21] to compute phase density and viscosity. The phase split occurs when the overall CO_2 composition is around 0.55 mol fraction. Our model accurately captures this phase split. The calculated data match the increasing liquid density trend in the single- and two-phase regions quite well. The agreement of calculated viscosity with measured data in single- and two-phase regions is also acceptable. We use the characterized fluid to saturate the slim tube to validate the MMP.

Other relevant data from Yellig and Metcalfe[26] are used to simulate the slim-tube experiment. These authors employ a stainless-steel tube with a length of 12.2 m and a diameter of 6.3 mm packed with 160−200-mesh sand. They report a permeability of approximately 2.47 × 10^{-12} m^2 (2.5 darcy) and pore volume of 85 cm^3. We use a constant injection rate of 3.6 cm^3/h[26] and carry out the simulation runs for pressures ranging from 8.4 to 18.8 MPa. Uniform initial composition and initial pressure are assumed. The oil recoveries at 1.2 pore volumes of injected (PVI) CO_2 are plotted for each pressure (Figure 3). A MMP of around 11.4 MPa is obtained. This is very close to the reported value for this oil sample. Lansangan and Smith[21] do not report other measurements related to fluid properties, such as saturation pressure, but we believe based on our matches on density, viscosity, and MMP that the characterized fluid in our model is representative of the original reported fluid.

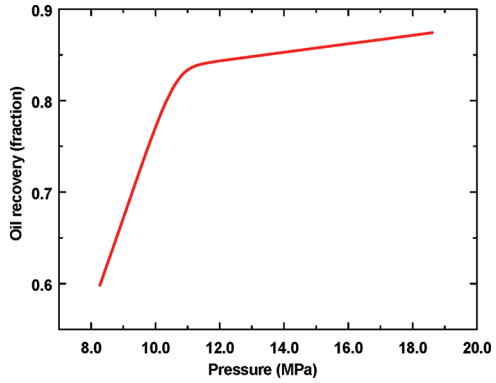

Figure 3. MMP validation of the characterized reservoir fluid RO-B in a slim tube simulation model. Simulated oil recoveries for different pressures are plotted at 1.2 PVI.

DENSITY EFFECTS IN THE 2D RESERVOIR CROSS-SECTION

To show the effect of density in the CO_2 flow path and oil recovery, we conduct a number of reservoir-scale simulations with two different density changes as CO_2 dissolves in the oil. The reference case has the default volume shift parameter (used in the commercial simulator), where there is a decrease in the oil density with CO_2 dissolution in the single phase. In the other case, we use the modified CO_2 shift parameter (as in Table 4), where the oil density increases with CO_2 dissolution (see Figure 1). In the following examples, a commercial compositional simulator (CMG GEM) with an IMPES scheme is used for simulations. We use a porosity of 22.35% for the following examples (except in example 2a). For time-stepping, we mostly use the default parameters in the CMG numerical

Table 6. Gas and Oil Relative Permeabilities

oil saturation	k_{ro}	k_{rg}
0.3	0	1
0.344	0.003	0.879
0.388	0.011	0.766
0.431	0.025	0.660
0.475	0.044	0.563
0.519	0.068	0.473
0.563	0.098	0.391
0.606	0.134	0.316
0.650	0.175	0.250
0.694	0.221	0.191
0.738	0.273	0.141
0.781	0.331	0.098
0.825	0.394	0.063
0.869	0.462	0.035
0.913	0.536	0.016
0.956	0.615	0.004
1	0.7	0

dx.doi.org/10.1021/ef300502f | Energy Fuels 2012, 26, 4590−4598

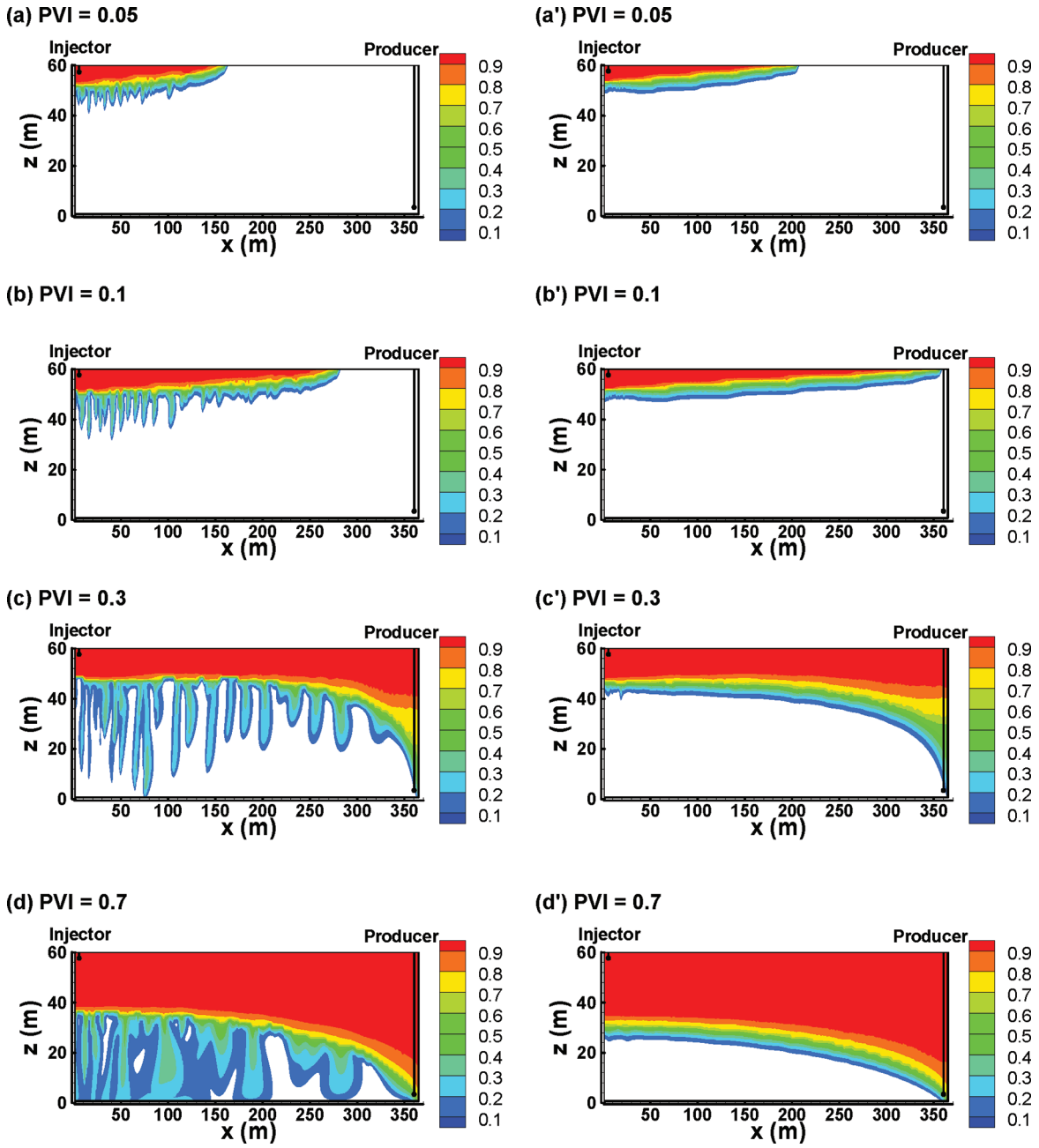

Figure 4. Overall CO_2 composition (mole fraction) at different PVI for (a, b, c, and d) increasing density with CO_2 dissolution and (a′, b′, c′, and d′) decreasing density with CO_2 dissolution: top, injection; bottom, production; homogeneous 2D media; and k = 1000 md.

simulator. There are some parameters in which their values have been modified. The list of these parameters and the values used in our simulations are shown in Table A1 of the Appendix. The material balance error values for the simulation results are in the order of 0.1%.

In all of the examples, the injection rate is constant (approximately 0.05 PV/year) and the pressure at the producing well is set equal to 11.7 MPa. The reservoir temperature for all of the examples is 46.7 °C. We do not consider initial water saturation in the examples. The gas and oil relative permeability data are listed in Table 6. In these examples, we observe a significant effect of increasing density with CO_2 dissolution on the flow path, time of breakthrough, and recovery. The examples presented here are limited to 2D domains. The 3D results are qualitatively similar to 2D results and will not be presented in this work for the sake of brevity. The 2D results are presented in the following two parts:

Part 1: Homogeneous Domain. *Example 1a: Top Injection in a 61.0 m Thick Reservoir.* We assume a domain with the length of 365.8 m (1200 ft), depth of 61.0 m (200 ft), and width of 5.0 m (16.4 ft). The injector well is located at the top left corner, and the producer is located at the bottom right corner. In our model, there are 240 grids in the x direction (length) and 40 grids in the z direction (depth). There is no gridding effect using such refined cells. In our simulations, we noted that the use of coarse grids may not result in the formation of fingers or it may cause a long delay in finger formation. This may have been one reason why finger formation from the density increase has not been reported in

dx.doi.org/10.1021/ef300502f | *Energy Fuels* 2012, 26, 4590−4598

the past in the study of the so-called gravity-stable CO_2 injection.

In this example, we use constant permeability of 1000 md. Figure 4 presents CO_2 composition profiles in the domain at 0.05, 0.1, 0.3, and 0.7 PV injection for both the default case (default CO_2 shift parameter) and the case with increasing oil density with CO_2 dissolution (modified CO_2 shift parameter). The results show the effect of the increasing density on the CO_2 composition in the flow path and front shape. There are two density effects: (1) increase in oil density with CO_2 dissolution (single-phase density effect) and (2) increase in liquid-phase density after the gas phase evolves in two phases. Both of these effects result in a heavier fluid (CO_2 + oil) to be placed on top of a lighter fluid (oil). This density difference in relatively high permeabilities can cause gravity instability, as shown in panels c and d of Figure 4. Note that, even when the single-phase density effect is neglected, there is the possibility of gravity instability because of gas evolution. A comparison of panels c and d to panels c′ and d′ of Figure 4 reveals that the single-phase density effect can significantly enhance the gravity instability at k = 1000 md.

If the producer well is located below the injector well, there will be an early breakthrough, as was the case for CO_2 injection in the Wellman field.[8] Injecting of CO_2 from the bottom creates different flow paths with and without the density effect from dissolution, because of large density differences usually observed between CO_2 and the oil phase. Most often CO_2 is lighter than the oil, and therefore, injection from the bottom is unattractive. When a reservoir is not thick, a strategy is to perforate the entire interval in the production and injection wells, as discussed in the next section.

Example 1b: Uniform Injection in a 30.5 m Thick Reservoir. To study the effect of reservoir thickness and injection/production scenarios, in this example, we use different dimensions from those of example 1a. The length of the 2D domain is doubled to 731.5 m (2400 ft), and the thickness is halved to 30.5 m (100 ft). Two cases for permeability are considered: 100 and 1000 md. The domain in this example is modeled by 480 grids in the x direction and 20 grids in the z direction. We performed various sensitivity studies to reduce the gridding effect. The reservoir pore volume and CO_2 injection rate are the same in all of our examples. The injector and production wells in this and the rest of the examples are completed along the depth of the domain. As in the previous example, the injection rate is constant (approximately 0.05 PV/year) and the pressure at the producing well (in the bottom) is set equal to 11.7 MPa.

We observe from Figure 5 that, for the case of 100 md, the density effect does not result in significant improvement in vertical sweep efficiency. There is a slight variation in the flow profile, but the overall impact on recovery is minimal. The relatively lower permeability limits the formation of fingers. We will shortly see that the difference in the recovery performance is much greater with the increasing density effect at a higher reservoir permeability.

When the permeability is increased to 1000 md, there is a pronounced gravity fingering when the increasing density is modeled (Figure 6). Without the density effect, there is no fingering (Figure 7). The higher permeability increases the progression of gravity fingers, when the density effect is included. Figure 8 presents the recovery plots for this example for the two permeabilities. There is a significant effect of liquid density change on the breakthrough time and recovery for the

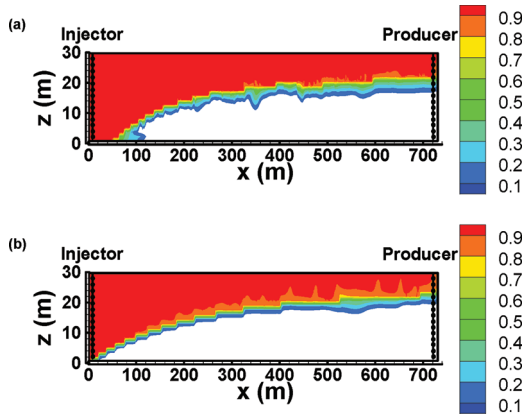

Figure 5. Overall CO_2 composition (mole fraction) at 0.7 PVI for (a) increasing density with CO_2 dissolution and (b) decreasing density with CO_2 dissolution (default): side wells; homogeneous media; and k = 100 md.

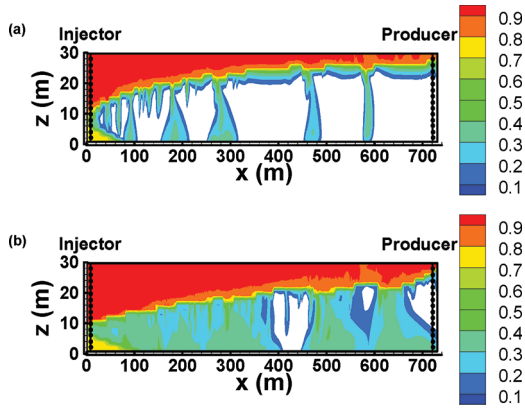

Figure 6. Overall CO_2 composition (mole fraction) at (a) 0.3 and (b) 0.7 PVI for increasing density with CO_2 dissolution: side wells; homogeneous media; and k = 1000 md.

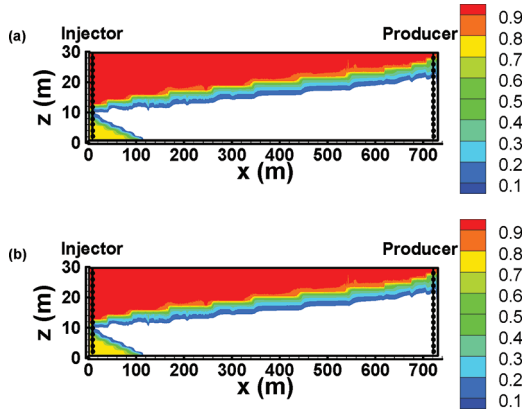

Figure 7. Overall CO_2 composition (mole fraction) at (a) 0.3 and (b) 0.7 PVI for decreasing density with CO_2 dissolution: side wells; homogeneous media; and k = 1000 md.

1000 md permeability. At 100 md, the effect of the density change from CO_2 dissolution in the liquid phase on recovery is small.

Part 2: Heterogeneous Domain. *Example 2a: Heterogeneous Permeability.* Using dimensions and the well pattern of example 1b, a heterogeneous domain with a permeability ranging from 10 to 1000 md is studied. The porosity in each

dx.doi.org/10.1021/ef300502f | Energy Fuels 2012, 26, 4590−4598

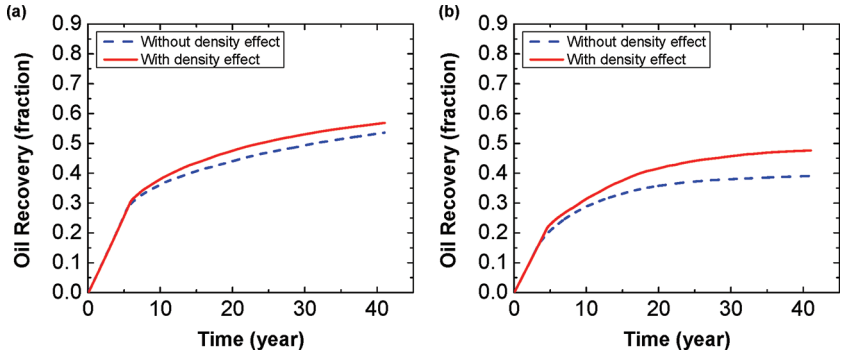

Figure 8. Oil recovery versus time with and without the density effect from CO_2 dissolution at (a) k = 100 md and (b) k = 1000 md: side wells.

grid block is related to permeability with the following logarithmic equation:[27] $\phi_i = 0.11889 + 0.2277 \log(k_i)$ (with k_i in millidarcies). The porosity and permeability distributions are shown in Figure 9. Figure 10 shows the overall CO_2 mole fraction at 70% PVI with and without the proper density effect. It can be observed that, in this highly heterogeneous domain, the inclusion of the density effects changes the CO_2 flow path. There are more gravity fingers when the density effect is included, as seen in Figure 10a. Note that the fingers in Figure 10b are due to the density increase from evaporation. With the proper density effect, the recovery after the injection of 1 PV is around 45%. When the density effect is not included, the final recovery is approximately 40%.

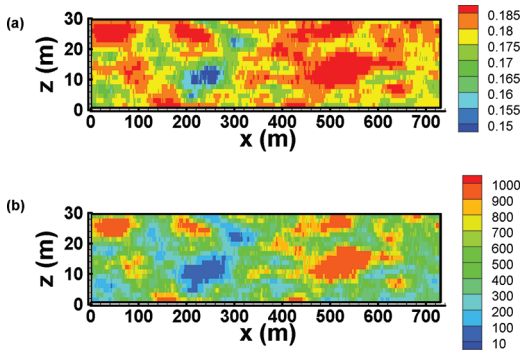

Figure 9. (a) Porosity and (b) permeability distribution for the 2D heterogeneous domain.

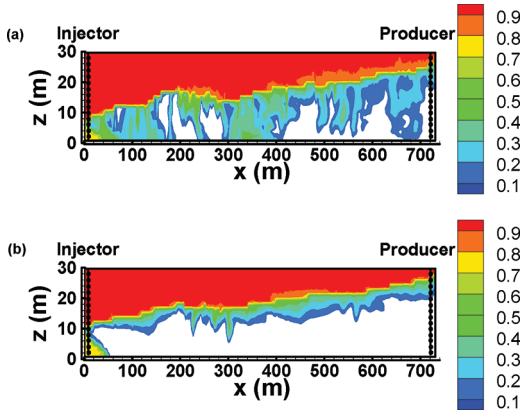

Figure 10. Overall CO_2 composition (mole fraction) at 0.7 PVI for (a) increasing density with CO_2 dissolution and (b) decreasing density with CO_2 dissolution (default): side wells and heterogeneous 2D media.

Example 2b: Anisotropic Permeability. The effect of permeability anisotropy is studied using the dimensions in example 2a. In a 2D domain with a horizontal permeability of 100 md, the k_v/k_h values of 0.1, 0.3, 0.5, and 1.0 are used in the simulations and the oil recoveries with time are compared with and without the proper density effect (Figure 11). It is observed that, for various degrees of anisotropy, the predicted oil recovery significantly reduces if the density effect is not included. The influence of the density effect on the flow path and recovery changes with vertical permeability.

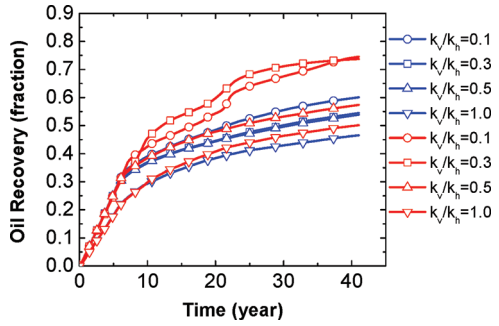

Figure 11. Effect of anisotropy on oil recovery versus time: side wells (blue, without the proper density effect; red, with the proper density effect).

SUMMARY AND CONCLUDING REMARKS

The central theme of this work relates to instability from the gravity effect because of the increase in oil density from CO_2 dissolution.

To capture the gravity effect, we should model the increase in oil density with CO_2 dissolution using the Peng–Robinson EOS. We show that, by changing the volume shift parameter of CO_2, one can model the increase in oil density with CO_2 dissolution. The Peng–Robinson EOS can predict the density of pure CO_2 by adjusting the CO_2 volume shift parameter. The use of the existing correlations for predicting the CO_2 volume shift parameters does not perform well for CO_2. Our analysis shows that, while the slim-tube MMP is independent of density effects, the oil density change from CO_2 dissolution can have a drastic effect on the recovery performance. Because of the 1D nature of flow in slim-tube experiments, the density effect is not taken into account. In reservoir conditions, when injected CO_2 is lighter than the oil phase, there may be no gravity-stable displacement because of the increase in oil density from solubility. CO_2 injection even when the density of the injected gas is less than the oil density may result in unstable gravity drainage. The literature in the past has neglected density effects

dx.doi.org/10.1021/ef300502f | Energy Fuels 2012, 26, 4590–4598

in the study and evaluation of CO_2 injection in the crest. We believe that the density measurement for CO_2/oil mixtures for different CO_2 compositions and the prediction of these results in the fluid model and proper reservoir simulation can significantly increase the reliability of the simulation results and decrease the degree of uncertainty. Heterogeneity may also have a significant effect, as expected. The location of injection and production wells may have a major impact on recovery.

APPENDIX

Numerical parameters of the GEM commercial simulator are provided in Table A1.

Table A1. Numerical Parameters in GEM for the Simulation Results

parameter	description	value
NORM PRESS	pressure change per time step (psi)	50
NORM SATUR	saturation change per time step	0.1
NORM GMOLAR	change in global composition per time step	0.1
DTMIN	minimum time-step size (day)	0.001
PRECC	convergence tolerance for the linear solver	1.0×10^{-4}
ITERMAX	maximum number of gmres iterations allowed in the Jacobian matrix solution routine	50
NORTH	maximum number of gmres steps to be performed in the iterative part of the linear equation solver before resetting	20
MAXRES	maximum scaled residual allowed for any single equation at convergence (tighter = 0.0001)	tighter

AUTHOR INFORMATION

Corresponding Author

*Telephone: (+974) 44230206. Fax: (+974) 44230011 E-mail: hadi.nasrabadi@qatar.tamu.edu (H.N.); abbas.firoozabadi@yale.edu (A.F.).

Notes

The authors declare no competing financial interest.

ACKNOWLEDGMENTS

This research is supported by the Qatar National Research Fund under Grant NPRP 29-6-7-30 and is greatly appreciated.

REFERENCES

(1) Sweatman, R. E.; Parker, M. E.; Crookshank, S. L. Industry experience with CO_2-enhanced oil recovery technology. *Proceedings of the Society of Petroleum Engineers (SPE) International Conference on CO_2 Capture, Storage, and Utilization*; San Diego, CA, Nov 2–4, 2009.

(2) United States Department of Energy (U.S. DOE). *Alabama Injection Project Aimed at Enhanced Oil Recovery, Testing Important Geologic CO_2 Storage*; U.S. DOE: Washington, D.C., 2010; http://www.fossil.energy.gov/news/techlines/2010/10004-CO2_Injection_Begins_in_Alabama_Oi.html.

(3) Hoteit, H.; Firoozabadi, A. Numerical modeling of diffusion in fractured media for gas-injection and -recycling schemes. *SPE J.* **2009**, *14* (2), 323–337.

(4) Perry, G. E. Weeks Island "S" sand reservoir B gravity stable miscible CO_2 displacement, Iberia Parish, Louisiana. *Proceedings of the Society of Petroleum Engineers (SPE) Enhanced Oil Recovery Symposium*; Tulsa, OK, April 4–7, 1982.

(5) Cardenas, R. L.; Alston, R. B.; Nute, A. J.; Kokolis, G. P. Laboratory design of a gravity-stable miscible CO_2 process. *J. Pet. Technol.* **1984**, *36* (1), 111–118.

(6) Palmer, F. S.; Nute, A. J.; Peterson, R. L. Implementation of a gravity-stable miscible CO_2 flood in the 8000 foot sand, Bay St. Elaine Field. *J. Pet. Technol.* **1984**, *36* (1), 101–110.

(7) Johnston, J. R. Weeks Island gravity stable CO_2 pilot. *Proceedings of the Society of Petroleum Engineers (SPE) Enhanced Oil Recovery Symposium*; Tulsa, OK, April 17–20, 1988.

(8) Bangia, V. K.; Yau, F. F.; Hendricks, G. R. Reservoir performance of a gravity-stable, vertical CO_2 miscible flood: Wolfcamp Reef Reservoir, Wellman Unit. *SPE Reservoir Eng.* **1993**, *8* (4), 261–269.

(9) Wo, S.; Yin, P.; Blakeney-DeJarnett, B.; Mullen, C. Simulation evaluation of gravity stable CO_2 flooding in the Muddy Reservoir at Grieve Field, Wyoming. *Proceedings of the Society of Petroleum Engineers (SPE)/Department of Energy (DOE) Symposium on Improved Oil Recovery*; Tulsa, OK, April 20–23, 2008.

(10) Jadhawar, P. S.; Sarma, H. K. Numerical simulation and sensitivity analysis of gas–oil gravity drainage process of enhanced oil recovery. *J. Can. Pet. Technol.* **2010**, *49* (2), 64–70.

(11) Moore, J. S. Design, installation, and early operation of the Timbalier Bay S-2B(RA)SU gravity-stable, miscible CO_2-injection project. *SPE Prod. Eng.* **1986**, *1* (5), 369–387.

(12) Nagai, R. B.; Redmond, G. W. Numerical simulation of a gravity stable, miscible CO_2 injection project in a west Texas carbonate reef. *Proceedings of the Society of Petroleum Engineers (SPE) Annual Technical Conference and Exhibition*; New Orleans, LA, Sept 26–29, 1982.

(13) Li, Z.; Firoozabadi, A. Cubic plus association equation of state for water containing mixtures: Is "cross association" necessary? *AIChE J.* **2009**, *55* (7), 1803–1813.

(14) Firoozabadi, A.; Cheng, P. Prospects for subsurface CO_2 sequestration. *AIChE J.* **2010**, *56* (6), 1398–1405.

(15) Farajzadeh, R. Enhanced transport phenomena in CO_2 sequestration and CO_2 EOR. Ph.D. Dissertation, Delft University of Technology, Delft, The Netherlands, 2008.

(16) Peng, D. Y.; Robinson, D. B. A new two-constant equation of state. *Ind. Eng. Chem. Fundam.* **1976**, *15* (1), 59–64.

(17) Lansangan, R. M.; Smith, J. L. Viscosity, density, and composition measurements of CO_2/west Texas oil systems. *SPE Reservoir Eng.* **1993**, *8* (3), 175–182.

(18) DeRuiter, R. A.; Nash, L. J.; Singletary, M. S. Solubility and displacement behavior of a viscous crude with CO_2 and hydrocarbon gases. *SPE Reservoir Eng.* **1994**, *9* (2), 101–106.

(19) Grigg, R. B. Dynamic phase composition, density, and viscosity measurements during CO_2 displacement of reservoir oil. *Proceedings of the Society of Petroleum Engineers (SPE) International Symposium on Oilfield Chemistry*; San Antonio, TX, Feb 14–17, 1995.

(20) Ashcroft, S. J.; Isa, M. B. Effect of dissolved gases on the densities of hydrocarbons. *J. Chem. Eng. Data* **1997**, *42* (6), 1244–1248.

(21) Lansangan, R. M.; Smith, J. L. *Supplement to SPE 21017, Viscosity, Density, and Composition Measurements of CO_2/West Texas Oil Systems*; Society of Petroleum Engineers (SPE): Richardson, TX, 1993; SPE Paper 26300.

(22) Pedersen, K. S.; Fredenslund, A. An improved corresponding states model for the prediction of oil and gas viscosities and thermal conductivities. *Chem. Eng. Sci.* **1987**, *42* (1), 182–186.

(23) Span, R.; Wagner, W. A new equation of state for carbon dioxide covering the fluid region from the triple point temperature to 1100 K at pressures up to 800 MPa. *J. Phys. Chem. Ref. Data* **1996**, *25* (6), 1509–1597.

(24) Jhaveri, B. S.; Youngren, G. K. Three-parameter modification of the Peng–Robinson equation of state to improve volumetric predictions. *SPE Reservoir Eng.* **1988**, *3* (3), 1033–1040.

(25) Lemmon, E.; McLinden, M.; Friend, D. Thermophysical properties of fluid systems. *NIST Chemistry Webbook, NIST Standard Reference Database*; National Institute of Standards and Technology (NIST): Gaithersburg, MD, 2005; 20899.

(26) Yellig, W. F.; Metcalfe, R. S. Determination and prediction of CO_2 minimum miscibility pressures. *J. Pet. Technol.* **1980**, *32* (1), 160−168 (includes associated paper 8876).
(27) Guyaguler, B. Optimization of well placement and assessment of uncertainty. Ph.D. Dissertation, Stanford University, Stanford, CA, 2002.